LA-UR -88-1446

CONF-880614--2

LA-UR--88-1446

DE88 010910

Los Alamos National Laboratory is operated by the University of California for the United States Department of Energy under contract W-7405-ENG-36

TITLE: **SOURCES OF POLARIZED IONS AND ATOMS**

AUTHOR(S): W. D. Cornelius

JUN 06 1988

SUBMITTED TO: 7th International Conference on Ion Implantation Technology, ITT'88 June 7-10, 1988, Tokyo, Japan

DISCLAIMER

Los Alamos
Los Alamos National Laboratory
Los Alamos, New Mexico 87545

FORM NO. 836 R4

SOURCES OF POLARIZED IONS AND ATOMS*

Wayne D. Cornelius
Accelerator Technology Division
Los Alamos National Laboratory, Los Alamos, NM 87545 USA

ABSTRACT

In this presentation we discuss methods of producing large quantities of polarized atoms and ions (Stern-Gerlach separation, optical pumping, and spin-exchange) as well as experimental methods of measuring the degree of polarization of atomic systems. The usefulness of polarized atoms in probing the microscopic magnetic surface properties of materials will also be discussed.

1. INTRODUCTION

Polarized ions have been available from polarized ion sources for nearly thirty years and have been used primarily in the examination of the spin-dependent terms in the nuclear interaction. It is only more recently that we have begun to apply polarized probes to the elucidation of microscopic electric and magnetic fields of materials' surfaces [1,2]. The concepts involved in the production of polarized probes are relatively simple. However, as we shall see, the production of intense polarized ensembles of atoms and ions is a complex process.

Because the nuclear magnetic moments are small, it is impractical to produce polarized nuclei directly. All of the practical techniques rely upon the hyperfine coupling between the electronic magnetic moments of unpaired atomic electrons and the nuclear magnetic moment. Hence, all sources of nuclear polarization have their roots in atomic physics. In what follows, I will discuss mainly the production of

*Work supported by the U. S. Department of Energy, Office of High Energy and Nuclear Physics.

polarized hydrogen ions because these sources make up the great majority of operational sources today. However, whenever the techniques can be applied to other atomic species, I will briefly cover that application as well.

2. THE LAMB-SHIFT SOURCE

The first practical polarized ion source utilized the Lamb-shift in the n = 2 levels of atomic hydrogen and its isotopes[3]. Figure 1 shows a Breit-Rabi diagram of the n = 2 levels of atomic hydrogen. The Lamb-shift, indicated in the figure, breaks the degeneracy of the n = 2 levels as shown leaving the metastable 2S level with slightly, higher energy than the 2P-1/2 level and somewhat lower energy than the 2P-3/2 level. As the magnetic field is increased, the energy levels shift as shown in the figure. Those levels with electronic spins aligned with the magnetic field increase in energy with increasing magnetic field. Those with antialigned electronic spins decrease in energy. At about 575 gauss, the lower 2S levels (historically called the beta states) cross the upper 2P-1/2 levels. Addition of a small electric field (1-10 V/cm) effectively mixes these levels and the beta states quickly transit to the ground state, leaving only the upper levels occupied (historically the alpha states). In the Lamb-shift source, the metastable beam is formed by a charge-capture reaction of protons with cesium vapor. Approximately one-third of the interacting protons are formed in the 2S levels. After the quenching of the beta states described above, the resulting atomic beam is passed into a cell containing argon gas. A near-resonance between atomic and ionic energy levels preferentially ionizes the n = 2 atoms to negative hydrogen ions. The ground-state atoms are only weakly ionized. Hence, the negative ion beam produced will have essentially the same nuclear polarization as the metastable atomic beam.

Following the 575-gauss field crossing and quenching of the beta states, the alpha states are atomically polarized (possess a net electronic spin orientation) but possess no net nuclear polarization. Therefore, before the argon cell, we must transform the atomic polarization into nuclear polarization. This is accomplished using a nonadiabatic reversal of the magnetic field[4]. Essentially, a "Sonatransition," as this technique is now called, utilizes a reversal of the magnetic field direction, which is rapid with respect to the Larmor precession rate of the atoms. Figure 2a is a Breit-Rabi diagram that demonstrates the details of the Sona-transition. At first we have only the F = 1 states with orientations of MF = + 1 and MF = 0, respectively (left side of the Fig. 2a). If the magnetic field is decreased rapidly to very low values (around 1

Gauss), the a_1 state cannot precess fast enough to follow the field. Therefore, when the magnetic field is subsequently reversed, the atomic spin remains fixed in a direction that is now opposite the applied magnetic field. This is equivalent to a transition from the a_1 state to the β_1 state. The a_2 state has MF = 0 and, thus, no preferred orientation along the magnetic field direction. Therefore, when the magnetic field reverses direction, the a_2 state simply turns itself inside out and continues to be an a_2 state.

If the magnetic field is again increased sufficiently above the critical field (where the nuclear coupling to the external field is equal to the hyperfine coupling), both nuclear spins will be antialigned with the external magnetic field and the electronic spins have no net alignment. Hence, the Sona-transition effectively transfers atomic spin orientation into nuclear spin orientation and subsequent ionization will provide a nuclear-polarized ion beam. Similar arguments can be used to demonstrate that if we start with only the beta states, the Sona-transition will again provide nuclear polarization (Fig. 2b). Transitions from the beta states cannot be used in the Lamb-shift source but, as we shall see, will play an important role in later polarized ion-source developments. One of the fundamental limitations of the Lamb-shift source is the rather low ion intensities available. Nature, it seems, has conspired to limit the ion currents available from the Lamb-shift source to approximately one microamp ere per ionized hyperfine level (for example, 2 microamperes from a source with a Sona-transition) [5].

3. ATOMIC-BEAM GROUND-STATE SOURCE

To increase the available polarized ion current, the atomic-beam, ground-state source was developed. In the ground-state source, hydrogen gas is dissociated and formed into a thermal, supersonic atomic beam that is passed through a multipole magnet. The interaction of the atomic magnetic moment with the magnetic field gradient of the multipole magnet produces a focusing force in those atoms with positive atomic spin projection (aligned with the magnetic field direction) and a defocusing force in those with negative projections. Hence, after a short distance, only the atoms with positive spin-projection remain in the beam. This Stern-Gerlach sepi ration technique has also been successfully used to produce beams of polarized alkali atoms [6,7] and polarized vapor targets [8].

Once again we have produced a beam of atoms polarized in electron spin and unpolarized in nuclear spin. The electronic polarization can now be transformed into

nuclear polarization as before. However, the beam velocities involved in the ground-state polarized source are low enough that it is difficult to meet the conditions of a Sona-transition; for example, the rate of change of the magnetic field is large compared with the rate of Larmor precession. In ground-state sources, nuclear polarization is achieved using rf transitions. By choosing the proper magnetic field and rf frequency, we can induce Majorana transitions between the hyperfine levels and induce nuclear polarization in the atomic beam.[9] The low velocities of the ground-state atomic beam reduce the longitudinal dimensions required for the rf transition to a practical size.

Because the ground-state source utilizes only ground-state atoms, selective ionization through a resonance (as in the Lamb-shift source) is not necessary. The original ground-state source ionizer concept used simple electron impact to produce H^+ and D^+ ions [10]. Subsequent improvements of the ground-state source have led to polarized ion currents in excess of 400 μA of H^+ and D^+ ions [11]. In order to produce negative ions from the ground-state source, two different concepts were developed into working sources. The first, developed by Gruebler et al. at ETH-Honggerberg, ues a conventional positive ion source and produces the negative ions by double charge exchange in sodium vapor [12]. To date this source has produced up to 16 μA of polarized H^- ions [11]. The alternative to the double charge-exchange concept, developed by Haeberli et al. at the University of Wisconsin [13] relies on direct ionization to H^- through interaction with a fast (40 keV) atomic cesium beam. This source has produced up to 40 μA of polarized H^- beam at the Brookhaven National Laboratory synchrotron [14].

4. Optically Pumped Sources

The final type of polarized ion source that I will discuss is the most recent development. With the recent improvements in high-power dye lasers, it has become possible to polarize a wide variety of atomic species by direct optical pumping [15]. Several of the optically pumped polarized ion source (OPPIS) ideas, both conceptual [16] and implemented into working models [7,17,18], utilize direct optical pumping of the atomic species of interest. A variation of the optical pumping theme uses charge exchange in an optically pumped vapor target [19,20].

Figure 3 shows schematically an OPPIS based on the charge exchange (CX) principle. Briefly, atomic polarization is achieved by capturing the polarized electron from the polarized vapor target. The atomic polarization is then

transformed into nuclear polarization by the Sona transition described earlier. The reversal of the polarization orientation is achieved by a reversal of the sense of the circular polarization of the laser photons and not by any physical change in the configuration of the source or its magnetic fields. As described earlier, the Sona transition is equally effective for initial alpha states or beta states in transforming atomic polarization into nuclear polarization. Optically pumped CX sources are on-line and/or under development at the Japanese National Laboratory for High Energy Physics in Tuskuba (KEK) [20], the Tri-University Meson Facility (TRIUMF) in Vancouver BC Canada [21], the Los Alamos Meson Physics Facility (LAMPF) in Los Alamos NM, USA [22], and the Soviet Institute for Nuclear Research (INR) near Moscow, USSR [23,24]. The source at KEK has produced up to 50 μA of polarized H^- beam [20] and the INR source has produced up to 1 mA of polarized H + beam [24].

More recently, the concept of spin exchange (SPX) has led to the possibility of polarizing atoms by direct spin-exchange with a polarized target rather than by a cx interaction [25]. The SPX concept is identical to the CX source except that no ions or ion beams are involved in the SPX source. Future development of the SPX source depends critically on achieving high polarizations in dense alkali vapor targets. Given the present rate of laser and target technology development, the SPX source should become available in the very near future [26,27].

The optically pumped source has been called the "universal polarized ion source" [15] because, in principle, it could be used to produce a polarized beam of any atomic species with nonzero nuclear spin. Hence, a wide variety of polarized probes can be made available for studying the properties of materials as outlined in Sec. 6.

5. Measurement Of Polarizations At Low Energies

Measurement of polarization at low energies has always been a problem. Nuclear polarization is easily determined by acceleration of ions up to several MeV and measuring asymmetries in a nuclear scattering experiment. This technique is most often impractical because a large accelerator facility is required.

In the type of laboratory experiments most often encountered, we have two different sets of conditions. We either have a well-collimated beam of atoms or we have an ensemble of atoms confined in some manner such as a vapor cell. These two conditions require different means of measuring polarizations.

If we have a beam of atoms and that beam of atoms is sufficiently dense, then the polarization of the ensemble can be measured by direct optical fluorescence. By tuning a single-mode laser ($\Delta f < 10$ MHz) through the absorption line(s) of the atoms, the strength of the fluorescence signal is proportional to the number density of the particular hyperfine state in resonance with the laser. The inherent directivity typical of atomic beams (for example, low transverse velocities) removes most of the Doppler broadening usually present in vapor targets. Therefore, we easily obtain sufficiently high resolution to resolve the different hyperfine states. This technique is particularly useful for atoms with large transition strengths to the ground-state (such as the alkali atoms). In this case, extremely small numbers of atoms are detectable using optical fluorescence [28].

The atomic polarization can also be determined by passing the atomic beam through a Stern-Gerlach magnet as described above [27]. The transmission through the magnet depends on whether the atomic spin projection is aligned or antialigned with the field.

An alternative to direct optical fluorescence was developed by Dreves et al. [29,30]. This technique exploits the fact that singly charged alkali ions have electronic configuration with $J = 0$ (in the ionic ground state). Capture of an unpaired, unpolarized electron from a thin foil often produces neutral atoms in excited atomic levels. The hyperfine interaction transfers some of the nuclear polarization to the unpaired electron. By measuring the polarization of the light emitted by the excited-state atom in transiting to the ground state, the polarization of the nucleus can be inferred. The analyzing powers of the various excited states are easily calculated assuming LS coupling and folding the time-dependent electronic polarization with the lifetime of the excited state [31]. Schuler et al. have extended this technique into the vacuum ultraviolet to measure the polarization of hydrogen atoms [32].

For an ensemble of atoms contained within a cell, the polarization can be determined in several different ways. The simplest way is to form a hole in the cell and allow some of the atoms to leak out and form an atomic beam, allowing the techniques described above to be used. However, the polarization of the atoms in the cell can also be determined directly, along with the integrated number density, from the Faraday rotation of the plane of linear polarization of a probe laser passing through the cell [33,34,35,36]. This effect depends on virtual absorption and re-emission of photons near the absorption line of the atomic species in the cell. The difference between the indices of refraction of the circularly polarized components of

the linearly polarized light leads to a phase shift between those components and, hence, a physical rotation of the plane of linear polarization. By measuring this rotation angle, the polarization as well as the number density of atoms in the cell can be determined.

A final method of determining the polarization of atoms in a cell exploits the properties of the negative hydrogen ion [37]. This ion only exists in one configuration with the electronic spins antialigned. Hence, by passing a polarized atomic hydrogen beam through the cell, the H^- current produced in the cell is proportional to the product of the hydrogenic polarization, the electronic polarization of the atoms in the cell, and the cross section for charge pickup from the atomic species in the cell. Alternatively, a fast proton beam can be used, and the H^- current is proportional to the square of the polarization of the atoms in the cell and the polarization capture efficiency of the reaction [37,38].

6. POLARIZED SURFACE PHYSICS

During the 1985 polarization conference in Osaka, D. Fick reported on a study of the surface properties of certain refractory metals using polarized lithium and sodium beams [1]. The vector polarization of a ^6Li beam was used as a probe of the microscopic magnetic fields of the metallic surfaces under study, and the nuclear quadrupole moment of a ^{23}Na beam was used as a probe of the microscopic surface electric field gradient.

Figure 4 shows a schematic of Fick's experimental arrangement [31]. Polarized atoms were directed onto a hot refractory metal surface where the atoms were ionized on the surface after some residence time, which depended on the temperature of the surface. The polarization of the emitted ions was measured using the beam-foil spectroscopic technique described above. The parameter measured was the depolarization of the incident lithium and sodium atoms and nuclei as a function of the surface temperature, external magnetic field, and incident polarization type (vector or tensor). Further, by applying rf fields at the surfaces under study, he was able to derive not only the magnitude and sign of the surface electric field gradient from the Stark-splitting of the nuclear magnetic resonance spectra, but also the asymmetry parameter, η, indicating the deviation of the electric field gradient from rotational symmetry around a normal vector to the surface (Table I) [31]. Fick's experimental technique is restricted to atomic species with low ionization energies

(the alkali atoms) absorbed on hot (1000°C) metallic surfaces with high work functions (the refractory metals). However, he does allude to an ongoing experimental program to measure the nuclear polarizations of desorbing atoms using laser-induced fluorescence [39].

More recently, Schmor et al. have used optical pumping to examine the microscopic magnetic surface properties of several materials that make up the containment walls of their sodium vapor target cell [2]. Figure 5 shows a schematic of their experimental apparatus. The sodium vapor is contained within the walls of a tube made of the various materials under test. The polarization of the sodium was monitored using the Faraday rotation method outlined above. By chopping the pump laser light, the decay of polarization with time could be determined. By examining the details of how the optically pumped polarization decays with time, they were able to deduce not only polarization relaxation times characteristic of different surfaces, but also microscopic magnetic field values at the surface (Table II). The TRIUMF experiments demonstrate the usefulness of polarized atoms in deducing surface magnetic fields. For example, macroscopically stainless steel is nonmagnetic. However, the microscopic domains have significant residual magnetic fields close to the surface (Table II). These microscopic fields are very efficient at depolarizing atoms by way of the magnetic dipole-dipole interaction. The copper metallic surface has somewhat reduced surface magnetic field strength. Coating either material with a mixture of methyl-trimethoxysilane and dimethyl-dimethoxysilane (dry-film) substantially reduces the microscopic magnetic fields evident at the surface (Table II).

7. CONCLUSION

As we have seen, the production of polarized atoms and ions has been simplified greatly in recent years with the introduction of intense, tunable dye lasers. Optically pumped polarized ion sources (both CX and SPX) should be capable of providing polarized atoms and ions of nearly all atomic species with nonzero nuclear, atomic, or ionic spins. The interaction of these spins with the microscopic electric and magnetic fields of surfaces leads to depolarization of the atoms and ions. By studying the details of the depolarization process, we can gather information about the microscopic electric and magnetic fields at the surface of a solid.

REFERENCES

[1] D. Fick, Proc. Sixth Int. Symp. on Polarization Phenom. in Nucl. Phys., Osaka, 1985 J. Phys. Soc. Jpn. 55 (1986) Suppl. p. 423-432..

[2] C. D. P. Levy, P. W. Schmor, and W. M. Law, $<S_z>$ Wall Relaxation Measurements of Optically Pumped Sodium Atoms at High Magnetic Field, Journal of Applied Physics, May 1988 (to be published).

[3] T. B. Clegg has written two excellent review articles on the Lamb-shift source: 1) Proc. Conference on Polarized Proton Ion Sources, Ann Arbor, MI, 1981, AIP Conf. Proc. 80 (1982) 21; 2) Proc. Conference on Polarized Proton Ion Sources, Vancouver BC, 1983, AIP Conf. Proc. 117 (1984) 63.

[4] P. G. Sona, Energ. Nucl. (Milan) 14 (1967) 295.

[5] P. Schiemenz, Helvitica Physica Acta, 59 (1986) 620.

[6] P. Egelhof, B. Bauer, R. Bottger, S. Kossionides, K. -H. Mobius, Z. Moroz, D. Presinger, R. Schuch, E. Steffens, G. Tungate, W. Dreves, I. Koenig, and D. Fick, Fifth International Symposium on Polarization Phenomena in Nuclear Physics, Sante Fe NM, 1985, AIP Conference Proceedings No. 69 (1981), p. 916.

[7] D. Kramer, E. Steffens, and T. Jansch, in Proceedings of the Workshop on Polarized Targets in Storage Rings, R. J. Holt ed., Argonne National Laboratory Report ANL-84-50 (1984), p. 155.

[8] W. Gruebler has written an excellent review of atomic beam polarized target technology in Proceedings of the Workshop on Polarized Targets in Storage Rings, R. J. Holt, ed., Argonne National Laboratory report ANL-84-50 (1984), p. 223.

[9] W. Haeberli, Ann. Rev. Nucl. Sci. 17 (1967)373.

[10] H. F. Glavish, Third International Symposium on Polarization Phenomena in Nuclear Physics, Madison WI, H. H. Barschall & W. Haeberli ed., (University of Wisconsin Press, 1971), p. 267.

[11] W. Gruebler, P. A. Schmelzback, D. Singy, and W. Z. Zhang, Helvitica Physica Acta, 59 (1986)568.

[12] P. A. Schmelzbach, W. Gruebler, V. Konig, and B. Jenny, Fifth International Symposium on Polarization Phenomena in Nuclear Physics, Sante Fe, NM, 1985, AIP Conference Proceedings No. 69 (1981), p. 899.

[13] W. Haeberli, M. D. Barker, G. Calkey, C. A. Gossett, D. G. Mavis, P. A. Quin, J. Sowinski, and T. Wise, Fifth International Symposium on Polarization Phenomena in Nuclear Physics, Sante Fe, NM, 1985, AIP Conference Proceedings No. 69 (1981), p. 877.

[14] A. Kponou, J. G. Alessi, A. Hershcovitch, T. O. Niinikoski, AIP Conference Proceedings No. 158 (1987), p. 585.

[15] D. E. Murnick and M. S. Feld, Fifth International Symposium on Polarization Phenomena in Nuclear Physics, Sante Fe, NM, 1985, AIP Conference Proceedings No. 69 (1981), p. 804.

[16] L. W. Anderson and G. A. Nimmo, Phys. Rev. Lett. 42 (1979) 1620.

[17] W. Dreves, W. Broermann, M. Elbel, W, Kamke, D. Fick, and E. Steffens, Fifth International Symposium on Polarization Phenomena in Nuclear Physics, Sante Fe, NM, 1985, AIP Conference Proceedings No. 69 (1981), p. 925.

[18] W. Dreves, W. Kamke, W. Broermann, and D. Fick, Z. Phys. A303 (1981) 203.

[19] L. W. Anderson, Nucl. Instr. & Meth. 167 (1979) 363.

[20] Y. Mori, A. Takagi, K. Ikegami, S. Fukumoto, A. Ueno, C. D. P. Levy, and P. W. Schmor, AIP Conference Proceedings No. 158 (1987), p. 605.

[21] M. Law, C. D. P. Levy, M. McDonald, P. W. Schmor, and J. Uegaki, AIP Conference Proceedings No. 158 (1987), p. 610.

[22] R. L. York, M. Dulick, W. D. Cornelius, and O. B. VanDyck, in Proc. International Workshop on Hadron Facility Technology, Santa Fe, NM, February 1987, H. A. Thiessen, ed., Los Alamos Conference report LA-11130-C, Los Alamos National Laboratory, p. 333.

[23] A. N. Zelenskii, S. A. Kokhanovskii, V. M. Lobashev, and V. G. Polushkin, JETP Letters 42 (1985) 5.

[24] A. N. Zelenskii, S. A. Kokhanovskii, V. M. Lobashev, V. G. Polushkin, and K. N. Vishnevskii, Helvitica Physica Acta, 59 (1986) 681.

[25] D. R. Swenson, D. Tupa, and L. W. Anderson, Helvitica Physica Acta, 59 (1986) 662.

[26] Y. Mori, A. Takagi, K. Ikegami, S. Fukumoto, A. Ueno, C. D. P. Levy, and P. W. Schmor, Nucl. Instr. & Meth. A (to be published) (KEK preprint 87-77, September 1987).

[27] A. Ueno, K. Ogura, Y. Wakuta, I. Kumabe, K. O-Ohata, Y. Mori, and S. Fukumoto, Nucl. Instr. & Meth. (to be published), (KEK preprint 87-164, March 1988).

[28] W. M. Fairbank, Jr., T. W. Hansch, and A. L. Schallow J. Opt. Soc. Am. 65 (1975) 199.

[29] H. J. Andra, H. J. Plohn, A. Gaupp, R. Frohling, Z. Physik A281 (1977) 15.

[30] W. Dreves, P. Egelhof, K. -H. Mobius, E. Steffens, G. Tungate, R. Bottger, D. Fick, Z. Physik A288 (1978) 413.

[31] B. Horn, E. Koch, and D. Fick, Phys. Rev. Lett. 53 (1984) 334.

[32] K. P. Schuler, C. J. Liu, and T. J. Gay, Helvitica Physica Acta, 59 (1986) 703.

[33] W. D. Cornelius, D. J. Taylor, R. L. York, and E. A. Hinds, Phys. Rev. Lett. 48 (1982) 870.

[34] Y. Mori, K. Ikegami, A. Takagi, S. Fukumoto, and W. D. Cornelius, Nucl. Instr. & Meth. 220 (1984) 264.

[35] Y. Mori, A. Takagi, K. Ikebami, S. Fukumoto, A. Ueno, C. D. P. Levy, and P. W. Schmor, AIP Conference Proceedings No. 158 (1987), 610.

[36] Z. Wu, M. Kitano, W. Happer, and J. Daniels, Appl. Optics 25 (1986) 4483.

[37] W. D. Cornelius, Workshop on Polarized Targets in Storage Rings, R. J. Holt ed., Argonne National Laboratory report ANL-84-50 (1984), 385.

[38] E .. Hinds, W. D. Cornelius, and R. L. York, Nucl. Instr. & Meth. 189 (1981) 599.

[39] U. Memmert, Ph. D. Thesis, Universitat Marburg, 1986.

Table I. Measured values of the electric field gradient component Vzz and asymmetry parameter n (NMR = nuclear magnetic resonance, NLM = nuclear level mixing, from Ref. 1).

Surface	Nucleus	Method	T(K)	Bo(mT)	Vzz (V/c^2m ($\times 10^{15}$)	η
W(110)	^{6}Li	NMR	1130	16.3	0.0(4)	---
	^{7}Li	NMR	1210	47.9	-1.1(1)	---
	^{23}Na	NMR	1290	111.6	-47.4(3)	0.07(1)
	^{23}Na	NLM	1360	---	-49.0(4)	0.08(2)
W-O	^{6}Li	NMR	1160	16.3	+3.08(8)	---
	^{7}Li	NMR	1265	47.9	+2.59(2)	---
	^{23}Na	NMR	1245	111.6	-46.8(1)	0.02(1)
	^{23}Na	NLM	1360	---	-49.8(1)	0.02(1)

Table II. Tabulation of local magnetic field and correlation time for different wall materials (LMF = local magnetic field, from Ref. 2).

Material	LMF (kG)	Correlation Time ($\times 10^{12}$ s)
316 Stainless steel	4.01 ± 0.13	6.6 ± 0.2
Copper	2.14 ± 0.07	19.4 ± 0.5
Dry-Film coated wall	0.48 ± 0.02	82.5 ± 2.2

Figure Captions

Fig. 1. Breit-Rabi diagram of the n = 2 levels in atomic hydrogen. The solid lines in the figure show the relative state energies as a function of the magnetic field. The Lamb-shift is marked on the vertical axis. Each line shown is really a doublet consisting of proton spin-up and proton spin-down states. The lower 2S levels (traditionally called the beta states) cross with the upper 2P levels at around 575 Gauss (arrow). In this magnetic field, a small transverse electric field will effectively mix the 2S and 2P levels, causing the immediate (<2 ns) transition of the beta states to the ground state. The upper 2S levels (traditionally called the alpha states) are unaffected.

Fig. 2. Breit-Rabi diagram of the energies of the hyperfine s-states of hydrogen as a function of the ratio of the external magnetic field (B) to the magnetic field produced by the orbiting electron at the position of the nucleus (Bc). By scaling in this manner, these diagrams for both ground-state and metastable hydrogen atoms. Initially the magnetic field is oriented along the direction of motion of the atoms (left side of the figures). The magnetic field decreases linearly from left to right, reversing direction in the center.

Figure 2a demonstrates the Sona transition for initial alpha states (labeled 1 and 2). The dotted lines show the occupied levels and the dashed lines show the unoccupied levels. After the field reversal, the atoms occupy only levels 2 and 3. These levels have opposite electronic spin orientation and equal nuclear orientation. Figure 2b demonstrates the Sona transition for initial beta states (labeled 3 and 4). After the field reversal, the atoms occupy only levels 1 and 4. These levels also have opposite electronic spins and equal

nuclear spins. Hence the field reversal has converted electronic polarization into nuclear polarization.

For an efficient Sona transition, the magnetic field should change rapidly with respect to the Larmor precession rate of the atoms in that field. Hence when the field reverses direction, the hyperfine states with zero projection along the magnetic field (states 2 and 4) are unaffected. Those hyperfine states with angular momentum projection aligned or antialigned with the field (states 1 and 3), cannot precess rapidly enough to follow the field reversal. Hence they remain fixed in space in a direction which is now opposite to the external magnetic field.

Fig. 3. Diagram of the KEK polarized ion source based on optical pumping and charge exchange. The proton beam is produced in an electron-cyclotron resonance (ECR) ion source and passed into a sodium vapor target cell which is optically pumped with a laser. The magnetic field reverses direction between the polarized sodium target cell and an unpolarized sodium target cell used to form negative ions by electron capture (the ionizing cell). This figure is from reference 20.

Fig. 4. Schematic diagram of the experimental apparatus of Horn, Koch, and Fick [31]. The polarized atoms were directed onto a hot refractory metal surface where they were subsequently ionized after a mean residence time which depended upon the surface temperature. Following deflection of the ions out of the atomic beam, the remaining polarization of the atoms was analyzed the ions using a beam-foil spectroscopic technique described in reference 30. This figure is from reference 31.

Fig. 5. Schematic diagram of the experimental apparatus of Levy, Schmor, and Law [2]. The sodium vapor was contained in a target cell with replacible wall materials. The sodium was optically pumped using a laser. The average polarization of the sodium vapor was determined from Faraday rotation [33, 34, 35, 36]. This figure is from reference. 2.

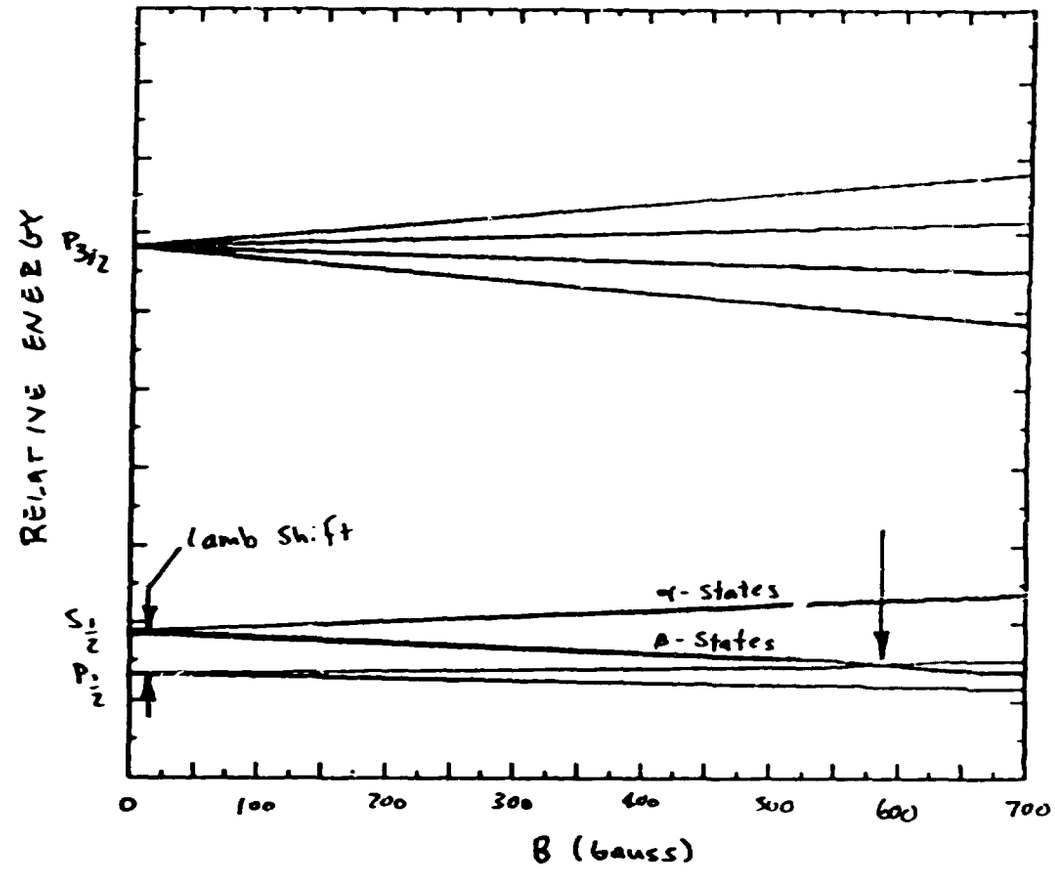
RELATIVE ENERGY
$P_{3/2}$
Lamb Shift
$S_{1/2}$
$P_{1/2}$
α - States
β - States
0
100
200
300
400
500
600
700
B (Gauss)

FIG. 1.

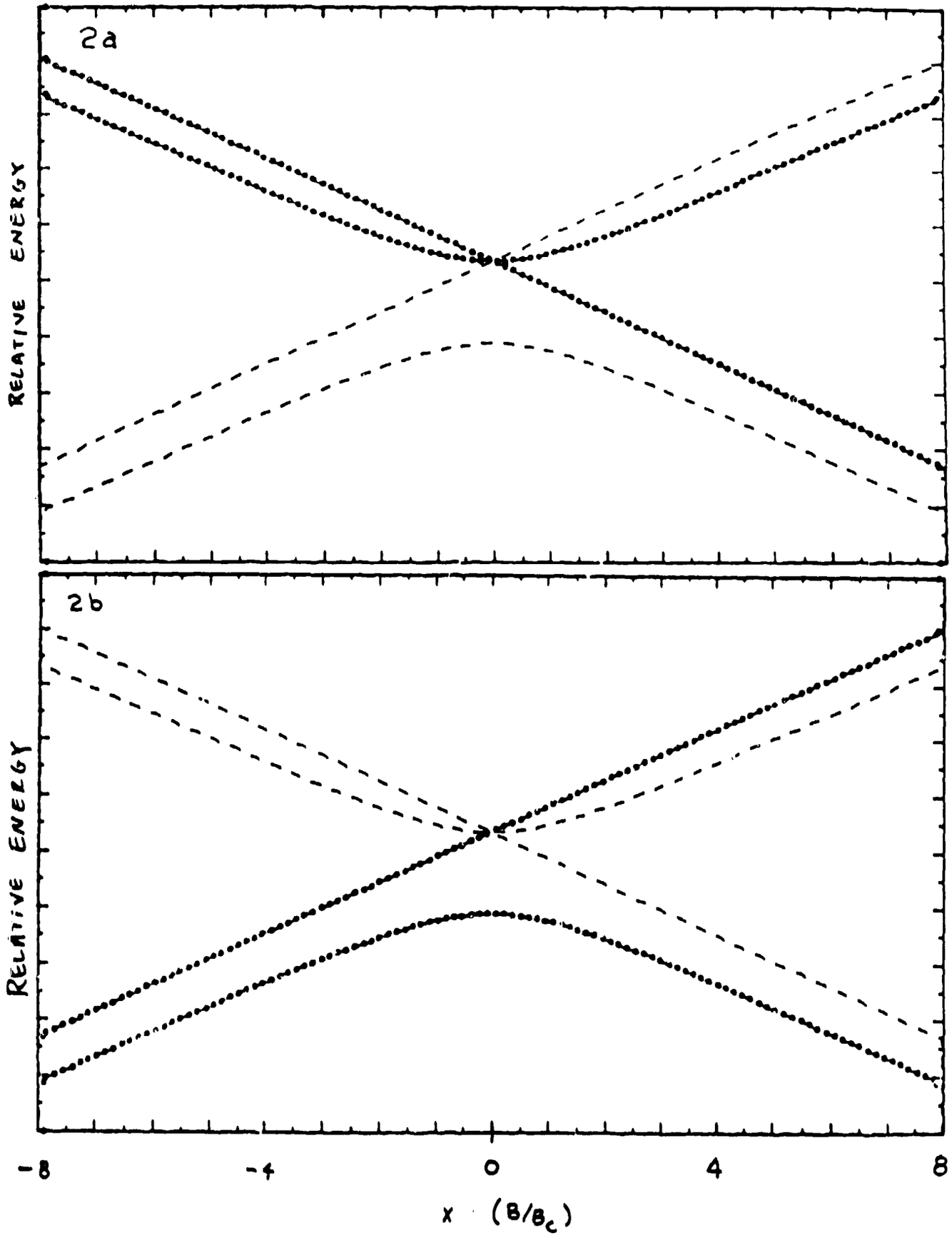

FIG. 2.

KEK POLARIZED H⁻ ION SOURCE

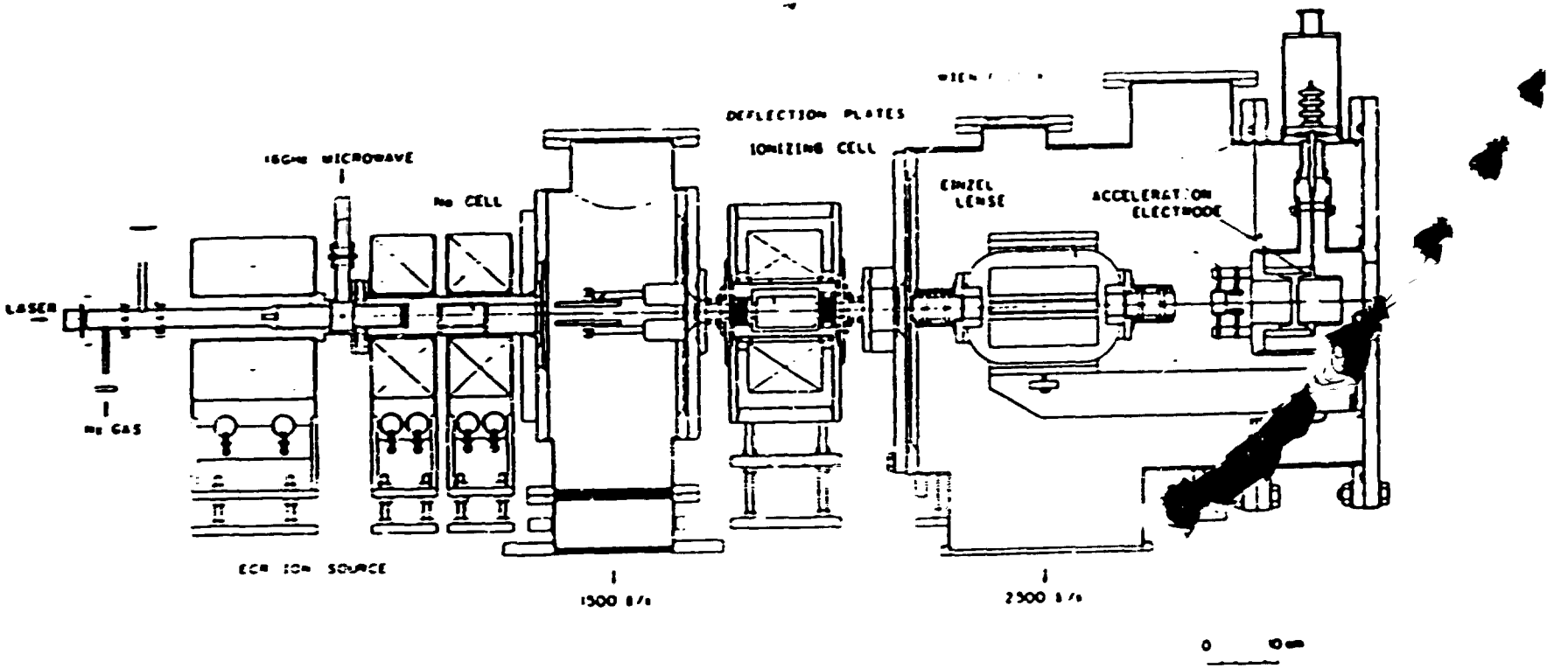

FIG. 3.

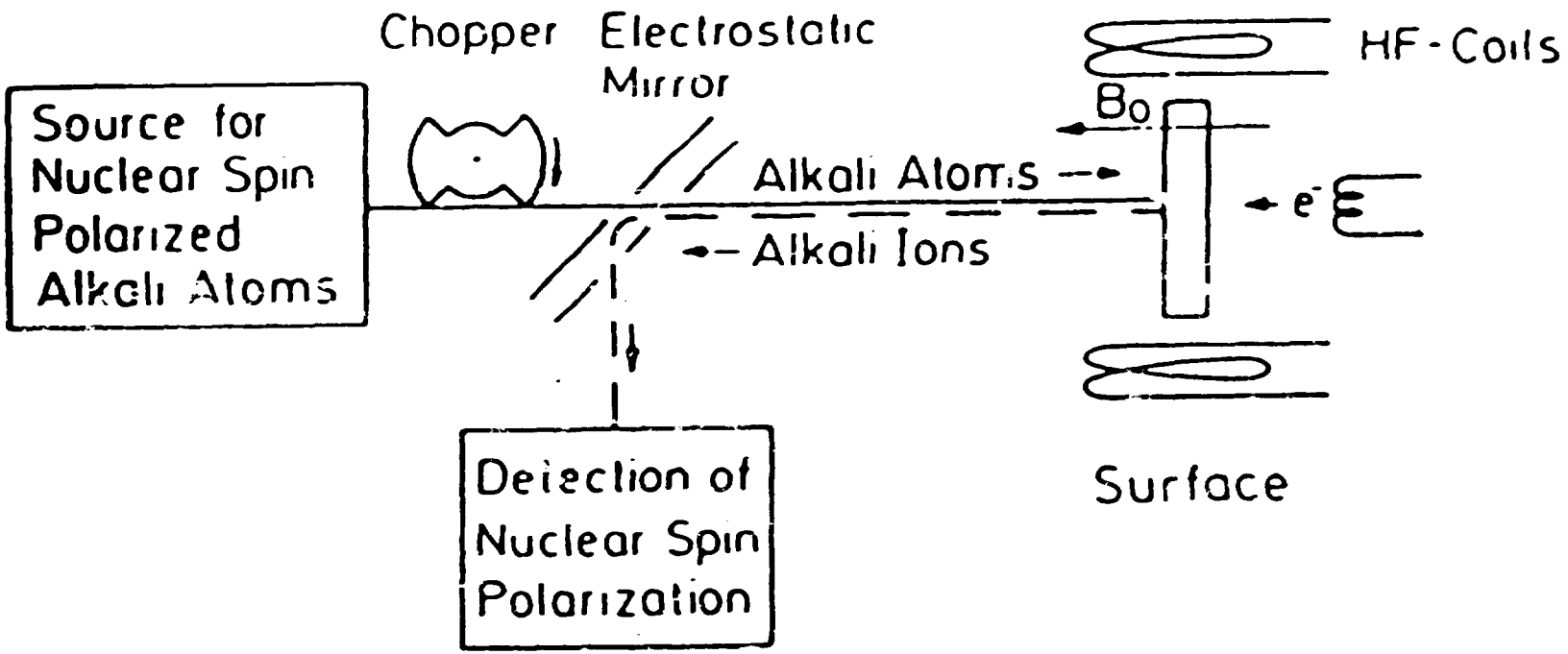
Chopper
Electrostatic Mirror
HF-Coils
Source for Nuclear Spin Polarized Alkali Atoms
B_0
Alkali Atoms
e^-
Alkali Ions
Detection of Nuclear Spin Polarization
Surface

FIG. 4

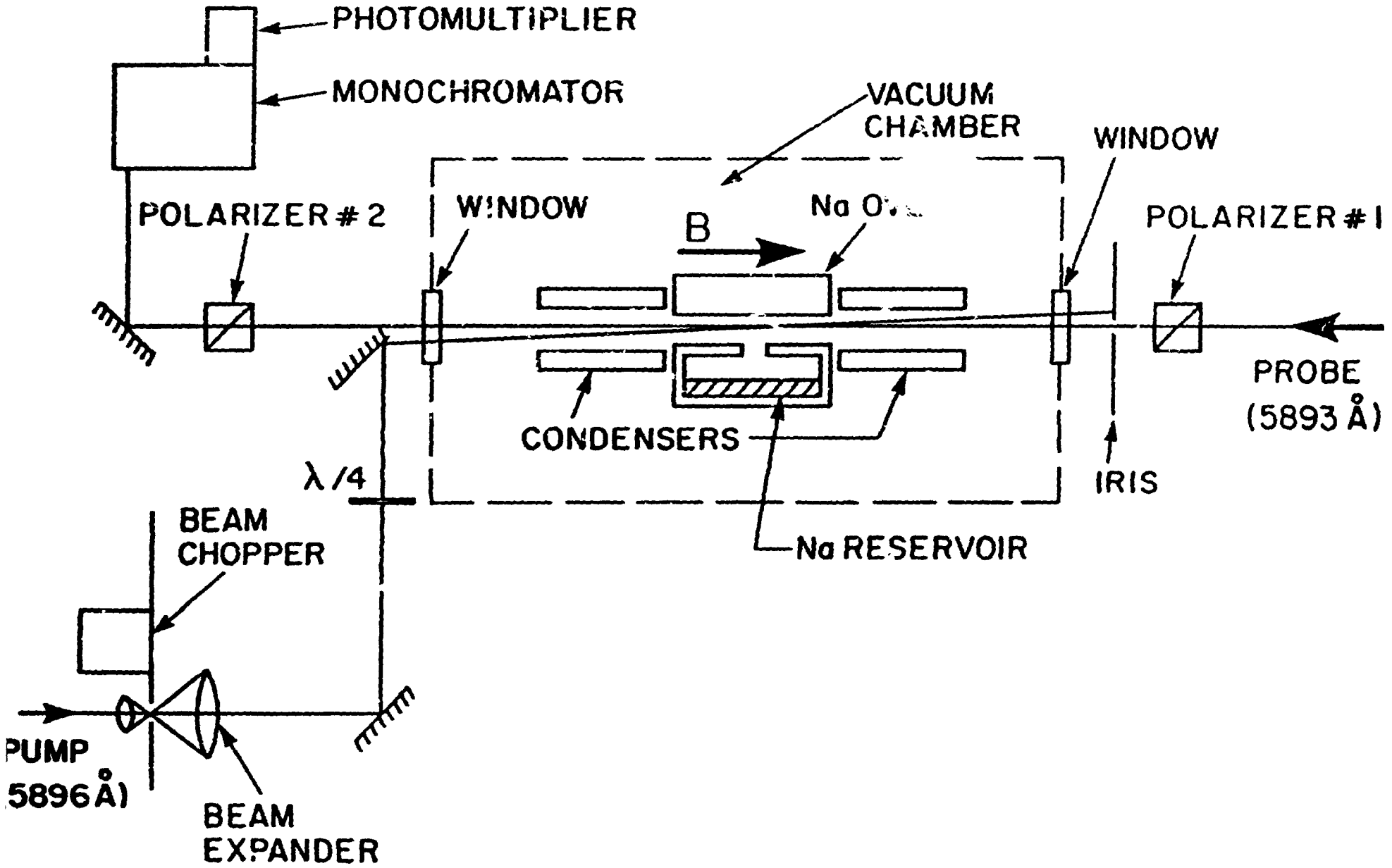
PHOTOMULTIPLIER
MONOCHROMATOR
VACUUM CHAMBER
WINDOW
POLARIZER #2
WINDOW
B
Na O
POLARIZER #1
PROBE (5893 Å)
CONDENSERS
λ/4
IRIS
BEAM CHOPPER
Na RESERVOIR
PUMP 5896 Å)
BEAM EXPANDER

FIG. 5.